AN APPLICATION OF THE METHOD OF CHARACTERISTICS
TO AXIALLY SYMMETRIC SUPERSONIC FLOW

Thesis by

Lt. Comdr. C. W. Griffing, U.S.N.
Lt. Comdr. W. C. Wilburn, U.S.N.
Lt. Comdr. D. Purdon, U.S.N.
Lt. Comdr. E. W. McLaughlin, U.S.N.

In partial fulfillment of the requirements for the
Professional Degree
in Aeronautical Engineering

California Institute of Technology
Pasadena, California
1947

ACKNOWLEDGEMENTS

TABLE OF CONTENTS

SUMMARY

The method of characteristics for three dimensional axially symmetric bodies was used to determine the velocity distribution about the nose of the Corporal E rocket, a rocket projectile, for Mach numbers 2 and 4. From the velocities the pressure distribution was determined and a drag coefficient computed.

For a starting point the nose of the projectile was approximated for a short distance by a cone and the Taylor-Maccoll* solution to this problem was used. This solution gave the angle of shockwave and the body. The Sauer graphical-numerical iteration method was used for the remainder of the solution.

Preliminary calculations and the work for Mach number 3 were carried out by Dr. H. K. Forster to whom we are indebted for instruction and aid with this work.

*Taylor, G. I. and Maccoll, J. W., Proc. Roy. Soc., A, Vol. 139, pp 278-311 1933.

CHARACTERISTICS*

The following discussion is for two dimensional flow and is taken from "Introduction to Aerodynamics of a Compressible Fluid", by H. W. Liepmann and Allen E. Puckett.

The term "characteristic" is related by definition to properties of certain partial differential equations. For any second order, partial differential equation of the type

$$(1) \quad A \frac{\partial^2 z}{\partial x^2} + 2B \frac{\partial^2 z}{\partial x \partial y} + C \frac{\partial^2 z}{\partial y^2} = D \frac{\partial z}{\partial x} + E \frac{\partial z}{\partial y} \cdots$$

two families of curves may be defined by the total differential equations

$$(2) \quad \frac{dy}{dx} = \frac{B \pm \sqrt{B^2 - AC}}{A}$$

where A, B, and C are functions of x and y. These curves (2) are known as the characteristics of equation (1).

These characteristics have certain properties which make them useful in an approximate solution process. These properties will be listed without proof:

1) They are invariant under transformation.

2) A solution $Z(x,y)$ to equation (1) may be composed of separate integral surfaces joining continuously with continuous derivatives along a line. This line is a characteristic. This property of the branching of integral surfaces along a characteristic permits us to regard the line as a wave front along which a disturbance is propagated through a field.

*Liepmann, H. W. and Puckett, Allen E. Introduction to Aerodynamics of a Compressible Fluid. pp 229-232 1947

3) Boundary conditions along any line, C, in the field will define a solution within a triangle bounded by C and the characteristics through the end points of C. Boundary conditions along a characteristic, however, will not define a solution in any region; boundary conditions must be given along two intersecting characteristics of different families. The exact equation of the velocity potential is:

$$(3) \quad (a^2 - u^2)\frac{\partial^2 \phi}{\partial x^2} - 2uv\frac{\partial^2 \phi}{\partial x \partial y} + (a^2 - v^2)\frac{\partial^2 \phi}{\partial y^2} = 0$$

where $\quad u = \frac{\partial \phi}{\partial x} \qquad v = \frac{\partial \phi}{\partial y}$

If a new dependent variable is defined

$$F(u,v) = ux + vy - \phi$$

then when a transformation is made to the hodograph plane, an element of the F surface in the (u,v) plane is defined by an element of the (x,y) surface. (Legendre Transformation). The transformation of equation (3) becomes

$$(4) \quad (a^2 - v^2)F_{uu} + 2uv F_{uv} + (a^2 - v^2)F_{vv}$$

The characteristics of the equation are

$$(5) \quad \frac{dv}{du} = \frac{\left(uv \pm \sqrt{u^2v^2 - (a^2 - u^2)(a^2 - v^2)}\right)}{(a^2 - v^2)}$$

This equation can be integrated immediately, "a" having been expressed as a function of u and v. Thus in the two dimensional case a characteristic chart may be constructed and is known as the "Prandtl-Busemann Characteristic Diagram."

When an attempt is made to use this method in three dimensional problems it is found that it cannot be done. A Legendre Transformation

leads to a non-linear equation in this case. In general, in three dimensional flow, it is not possible to construct a characteristic diagram. Instead, a separate construction must be carried out for each flow.

SAUER METHOD

The Sauer solution of supersonic axially symmetric flow is a graphical-numerical iteration method.

For a non-viscous, steady, isentropic flow of a perfect fluid without body forces, the equation of motion may be obtained by eliminating the pressure and density from the force equations and the equation of continuity. Transformed to cylindrical coordinates, and assuming axial symmetry, this becomes

$$(6) \quad \left(1 - \frac{u^2}{a^2}\right)\frac{\partial u}{\partial x} + \left(1 - \frac{v^2}{a^2}\right)\frac{\partial v}{\partial \lambda} - uv\left(\frac{\partial u}{\partial \lambda} + \frac{\partial v}{\partial x}\right) + \frac{v}{\lambda} = 0$$

Assuming irrotational flow the velocity components may be replaced by the proper derivatives of the velocity potential ϕ.

In the axially symmetric case, given a velocity vector, V, one can introduce in an axial plane a set of orthogonal axes in which X' is along the velocity vector. Then $u' = V$ and $v' = 0$ where u' is the velocity in the X' direction and v' is the velocity in the Y' direction.

If at a particular point the X', Y' coordinates are introduced equation (6) becomes

$$\left(1 - \frac{u^2}{a^2}\right)\frac{\partial u'}{\partial x'} + \frac{\partial v'}{\partial y'} + \frac{v}{\lambda} = 0$$

and introducing ϕ, for irrotational flow

$$(7) \quad \left(1 - \frac{v^2}{a^2}\right)\frac{\partial^2 \phi}{\partial x'^2} + \frac{\partial^2 \phi}{\partial y'^2} + \frac{1}{\lambda}\frac{\partial \phi}{\partial \lambda} = 0$$

The Mach angle is defined as $\alpha = \sin^{-1}\frac{V}{a}$ where a is the local speed of sound and V the local fluid velocity. A Mach line is a line inclined to the direction of fluid flow by an angle equal to the Mach angle.

At a point, where the velocity is known two Mach lines may be drawn. In this case where the velocity is along the X' axis, one Mach line will be at an angle $+\alpha$ and one at an angle $-\alpha$ from the X' axis. (See Fig. 1 a).
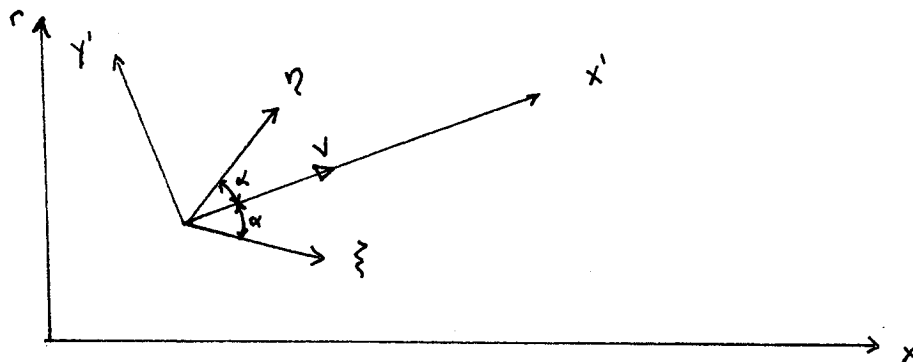
Fig. (1) a

These Mach lines, which may be identified as the character-istics of equation (6) define a new set of coordinate axes, ξ and η.

From the definition of the Mach angle, $\sin \alpha = \frac{a}{V}$ it is seen that substituting this in equation (7) we get

$$(8) \qquad \cot^2 \alpha \, \frac{\partial^2 \phi}{\partial X'^2} - \frac{\partial^2 \phi}{\partial Y'^2} = \frac{1}{\lambda} \frac{\partial \phi}{\partial \lambda}$$
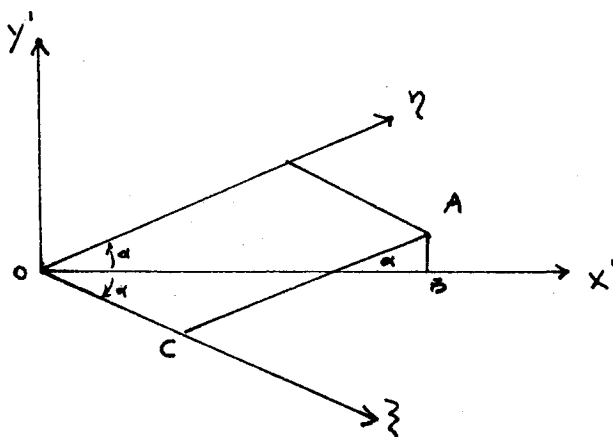

Fig. (1) b

$$\overline{OB} = X' = \overline{OC}\cos\alpha + \overline{CA}\cos\alpha = (\zeta+\eta)\cos\alpha \left.\right\}\ \text{FROM Fig 1(b)}$$

$$\overline{AB} = Y' = -\overline{OC}\sin\alpha + \overline{CA}\sin\alpha = (-\zeta+\eta)\sin\alpha$$

HENCE:
$$\zeta = \frac{1}{\sin 2\alpha}(X'\sin\alpha - Y'\cos\alpha) \quad \text{AND} \quad \eta = \frac{1}{\sin 2\alpha}(X'\sin\alpha + Y'\cos\alpha)$$

$$\frac{\partial\phi}{\partial x'} = \frac{\partial\phi}{\partial\zeta}\frac{\partial\zeta}{\partial x'} + \frac{\partial\phi}{\partial\eta}\frac{\partial\eta}{\partial x'} = \frac{1}{\sin 2\alpha}\left(\sin\alpha\frac{\partial\phi}{\partial\zeta} + \sin\alpha\frac{\partial\phi}{\partial\eta}\right) = \frac{1}{2\cos\alpha}\left(\frac{\partial\phi}{\partial\zeta} + \frac{\partial\phi}{\partial\eta}\right)$$

$$\frac{\partial\phi}{\partial y'} = \frac{\partial\phi}{\partial\zeta}\frac{\partial\zeta}{\partial y'} + \frac{\partial\phi}{\partial\eta}\frac{\partial\eta}{\partial y'} = \frac{1}{\sin 2\alpha}\left(-\cos\alpha\frac{\partial\phi}{\partial\zeta} + \cos\alpha\frac{\partial\phi}{\partial\eta}\right) = \frac{1}{2\sin\alpha}\left(-\frac{\partial\phi}{\partial\zeta} + \frac{\partial\phi}{\partial\eta}\right)$$

$$\frac{\partial^2\phi}{\partial x'^2} = \frac{1}{4\cos^2\alpha}\left(\frac{\partial^2\phi}{\partial\zeta^2} + \frac{\partial^2\phi}{\partial\eta^2} + 2\frac{\partial^2\phi}{\partial\zeta\partial\eta}\right)$$

$$\frac{\partial^2\phi}{\partial y'^2} = \frac{1}{4\cos^2\alpha}\left(\frac{\partial^2\phi}{\partial\zeta^2} + \frac{\partial^2\phi}{\partial\eta^2} - 2\frac{\partial^2\phi}{\partial\zeta\partial\eta}\right)$$

substituting these relations in (8)

$$\frac{\partial^2\phi}{\partial\eta\partial\zeta} = \frac{\sin^2\alpha}{\lambda}\frac{\partial\phi}{\partial\lambda}$$

This equation can be written

(9)
$$\frac{\partial}{\partial\zeta}\left(\frac{\partial\phi}{\partial\eta}\right) = \frac{dq}{d\zeta} = \frac{\sin^2\alpha}{\lambda}v$$

$$\frac{\partial}{\partial\eta}\left(\frac{\partial\phi}{\partial\zeta}\right) = \frac{dp}{d\eta} = \frac{\sin^2\alpha}{\lambda}v$$

where p and q indicate the projections of the velocity vector along

the ζ and η directions respectively.

Replacing the derivatives of (9) by a quotient of increments

and clearing fractions the equations become

(10)
$$dq = \frac{v}{\lambda}\sin^2\alpha\, d\zeta$$

$$dp = \frac{v}{\lambda}\sin^2\alpha\, d\eta$$

$d\zeta$ and $d\eta$ being the increments in the directions of the Mach lines

and dp and dq the projections of the velocity increment upon the

Mach lines.

PROCEDURE

The properties of the characteristics enable us to make an approximate solution. The mechanical process is a simultaneous construction of velocities in the hodograph plane and of Mach lines in the physical plane. Step by step small areas in the physical plane correspond to points in the hodograph plane since the flow field in the physical plane is divided into a finite number of small regions bounded by Mach lines over which averages are taken for computing velocities in the hodograph plane. Hence the accuracy of the computation will depend on the size of the regions bounded by Mach lines. The boundary conditions in the physical plane determine the direction of the velocity in the hodograph plane; at the shock wave the magnitude is also determined. The points in the hodograph plane when found by an iteration process based on estimates will in turn determine the Mach lines in the physical plane.

The two boundaries which define the boundary conditions are the shock wave attached to the nose and the surface of the body. Between these boundaries a net of Mach lines is constructed by proceeding from point to point until, in the entire area about the body and at points along the surface, the velocities are determined. This Mach net is shown in Fig. (5), Fig. (6) or Fig. (7).

The angle of the shock wave at the nose is obtained from Taylor-Maccoll solution of flow about a cone with the same nose angle. For this purpose, depending upon the geometry of the body the assumption that the nose is conical will be good at least a

small distance back from the vertex. Taylor and Maccoll showed that velocity magnitudes and directions are constant in super- sonic flow about a cone along radial lines through the vertex. This solution furnishes as many points as needed to start the characteristic method solution. These points can be taken close enough to the vertex to make the conical flow assumption valid.

With the boundaries established and some points in the phys- ical plane for which the velocities are known one may proceed by using the Sauer graphical method for computing supersonic axially symmetric flow. There are three different geometrical cases for which slightly different procedures are necessary. The cases are:

(a) from the known solution in two points in the free stream to calculate the solution in a third point in free stream;

(b) from the known solution in a point in the free stream to calculate the solution in a point on the body;

(c) from the known solution of a point on the shock wave and a point in the free stream to calculate the solution in a third point on the shock wave.

First, take the case of all points in the free stream. (see Fig. 2). Suppose points P_1 and P_2 are known: to find P_3, P_3' is estimated in the hodograph plane. Then with mean values, magnitude and direction, which are estimated, draw an average ζ_{13} and η_{23} line. Their intersection gives P_3 in the physical plane from which values are obtained for $d\zeta$, $d\eta$ and λ. With these values one can calculate dq and dp from

$$dq = \sin^2 \alpha \; \frac{v}{\lambda} \; d\zeta$$

$$dp = \sin^2 \alpha \; \frac{v}{\lambda} \; d\eta$$
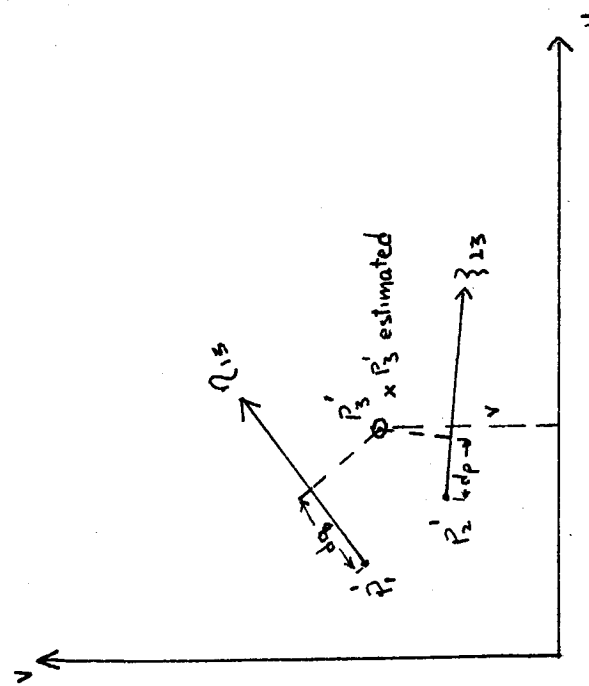
Physical Plane

Hodograph Plane
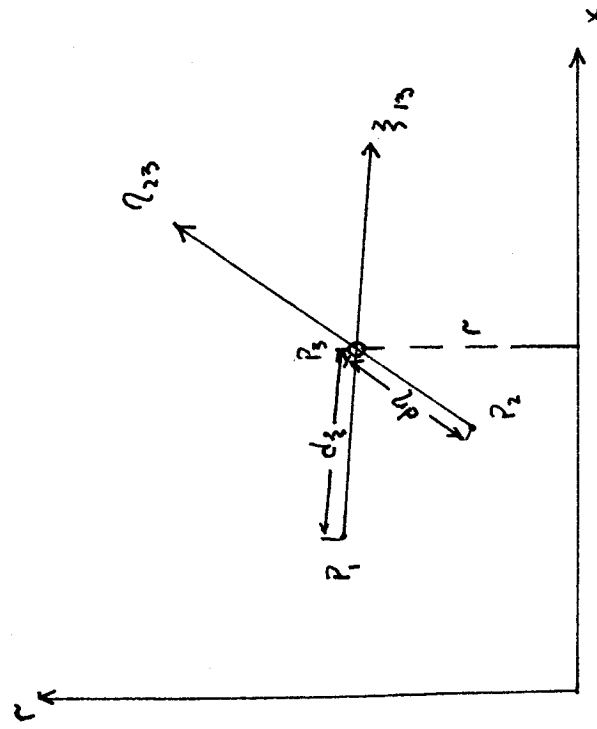
Fig. (2)

Then stepping off dq in the η_{13} direction and dp in the ζ_{23} direction perpendiculars are erected as shown in Fig. (2). These intersect in a point which will be very close or right on the estimated P_3'. If this is not within the desired accuracy the process is repeated until the iteration shows no change. Table I shows several examples of calculations made in obtaining the values necessary to construct Fig. (2).

For the case of obtaining a point on the surface of the body from a point in the free stream the procedure differs slightly. Referring to Fig. (3) suppose P_1 is known; P_2 is to be found. A ζ line, whose direction is estimated, is drawn from P_1 until it intersects the boundary at B. Since the flow is tangent to the boundary at all points on the boundary the direction of the flow velocity at point B is known, and an estimate of the magnitude of the flow velocity is made. From the mean between this estimated velocity and the velocity at P_1 a Mach angle is calculated. Similarly a mean value of the angle of flow direction (between P_1 and point B on the surface) is calculated. The difference between these two angles gives a new ζ line intersecting the boundary at $_1P_2$. The points P_1 and $_1P_2$ give the values necessary to calculate dq as in the free stream case. As before the construction is made in the hodograph plane and the perpendicular at a distance dq from P_1' along the η line intersects w_2 at $_1P_2'$. From the mean values of P_1' and P_2' draw the corresponding ζ line from P_1 in the physical plane. This should intersect the boundary at $_1P_2$. If not, one takes the tangent to the boundary at the new point and proceeds as

before. The velocities from successive points along the body fall, however, in a smooth curve in the hodograph plane making estimation easy with the result that the process generally does not need to be repeated.

Now in obtaining a point on the shock wave from a preceding point on the shock wave and a point in the free stream it must be noted that the angle of the shock wave is not known. The shock wave is conical only for flow about a cone. For a curved profile the shock wave is also a curve which for this method is approximated by a series of straight lines, the angles of which must be found. To do this the Busemann shock polar is used in the hodograph plane. The shock polar graphically expresses the relation between the velocity direction and magnitude of the downstream flow and the angle of the shock wave for a given free stream velocity. Referring to Fig. (4) suppose P_1 and P_2 are known; P_3 is to be found. Since P_3 is on the shock wave it is also on the shock polar along with P_1'' which is known. Estimate P_3' on the shock polar. The angle of the shock wave in the physical plane is the complement of the mean of $\angle OAP_1$ and $\angle OAP_3$. The η line P_2P_3 is obtained as in the free stream case. The intersection of this η line with the shock wave gives the values necessary to calculate dp. The construction in the hodograph plane is made giving the point P_3' at the intersection of the shock polar with the perpendicular to the ζ line from P_2'. Since the shock wave and the η line from P_2 are nearly parallel it is often necessary to repeat the procedure.

Physical Plane

Hodograph Plane

Fig. (3)

Physical Plane
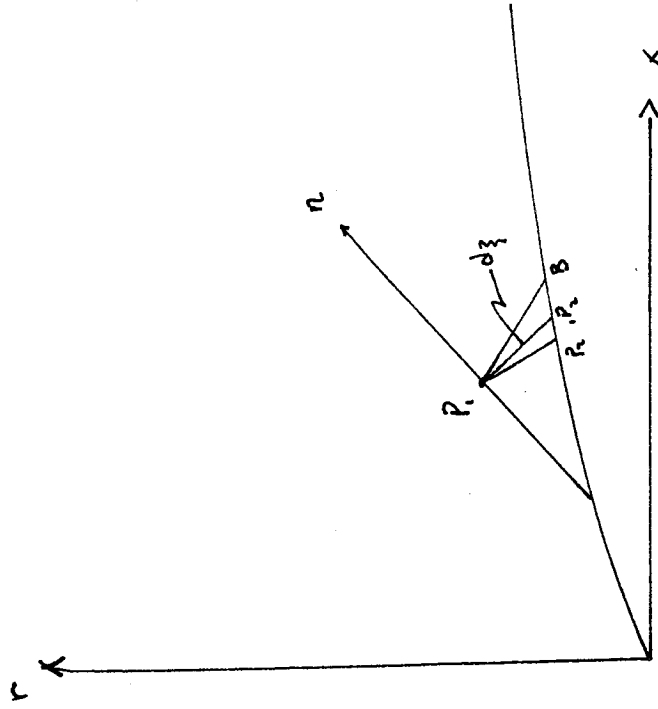
Hodograph Plane
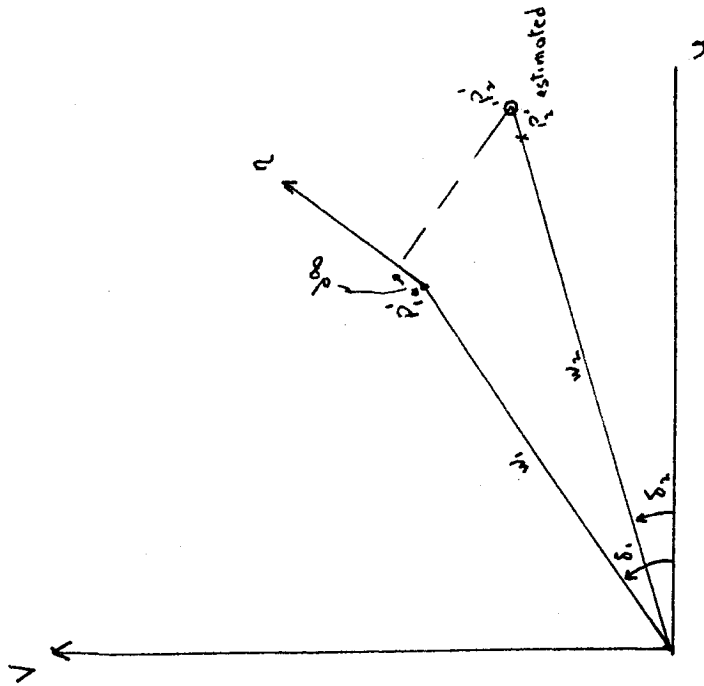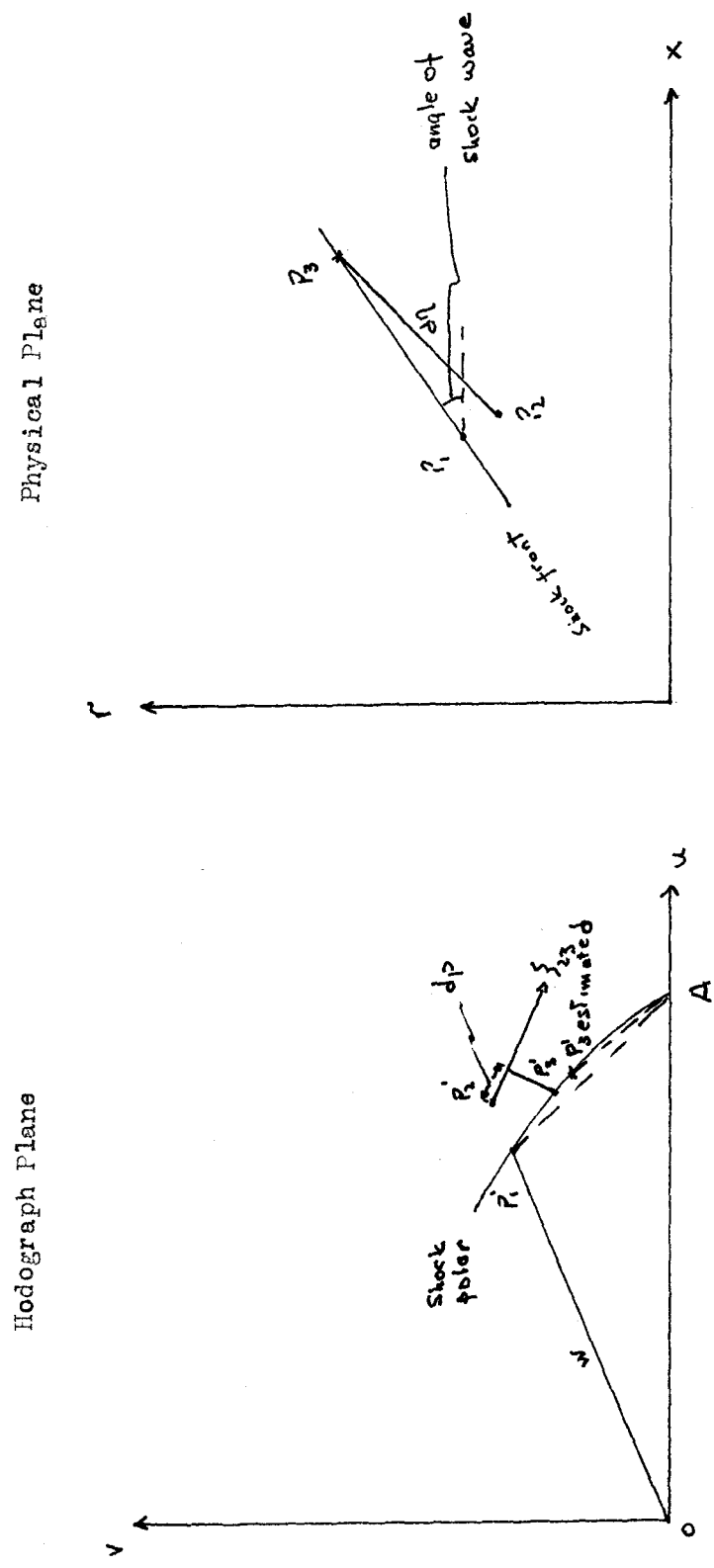
Fig. (4)

CALCULATION OF C_p AND C_D

After the calculation of the flow velocities is completed, all of the points of the Mach net between the shock wave and the surface of the body are tabulated, i.e., the geometrical position of the point and the stream velocity at the point. (see Table II). In the calculation of the drag of the nose section, however, only the points on the surface of the missile are needed. Given a number of points on the surface and the velocities at these points the pressure coefficient, C_p, is computed for each of these points and a plot is made of C_p vs. X. (see Fig. (8)). From this curve values of C_p are obtained for regular increments of X and then by carrying out the appropriate integration (in this case a graphical integration was used; see Fig. (10)) the drag coefficient, C_D, can be obtained for the nose of the missile.

The equations used in the actual computations are discussed below:

In general

$$C_p = \frac{p - p_1}{\frac{1}{2}\rho w^2} = \frac{\frac{p}{p_0} - \frac{p_1}{p_0}}{\frac{\rho w^2}{2 p_0}}$$

and

$$\frac{\rho w^2}{2} = \frac{\gamma p}{2} \frac{\rho w^2}{\gamma p} = \frac{\gamma p}{2} \frac{w^2}{a^2} = \frac{\gamma p}{2} M_1^2$$

where M_1 is the free stream Mach Number.

$$C_p = \frac{\frac{p}{p_0} - \frac{p_1}{p_0}}{\frac{\gamma p_0}{p_0} M_1^2}$$

Across the shock wave, however, there is a drop in stagnation pressure. This drop is defined by $z = p_3/p_0$ where p_3 corresponds to stagnation conditions behind the shock wave and p_0 corresponds to free stream stagnation conditions.

Then,
$$C_p = Z \frac{\frac{p}{p_0} - \frac{p_1}{p_0}}{\frac{\gamma M_1^2}{2} \frac{p_1}{p_0}}$$

Z is a function of the strength of the shock wave and thus of the shock wave angle, which is known from the Taylor-Maccoll solution (the angle of the shock wave is taken at the nose), and of the free stream Mach number.

Given M_1 and α (see figure below) Z is computed as follows[*]:

1. $$M_1^2 = \frac{2}{\gamma - 1} \left[\left(\frac{1}{Z}\right)^{\frac{\gamma-1}{\gamma}} - 1 \right]$$

2. $$\cos^2 \alpha = \frac{\left[(\gamma-1) + (\gamma+1)\left(\frac{\gamma}{Z}\right) \right](\gamma-1)}{4\gamma\left[\left(\frac{1}{Z}\right)^{\frac{\gamma-1}{\gamma}} - 1 \right]}$$

3. $$\frac{\tan \beta}{\tan \alpha} = \frac{(\gamma-1) + (\gamma+1)\left(\frac{\gamma}{Z}\right)}{(\gamma+1) + (\gamma-1)\left(\frac{\gamma}{Z}\right)}$$
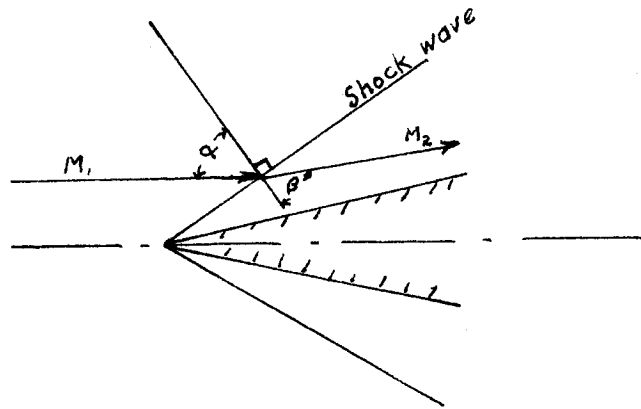
[*]Durand, W. F., Aerodynamic Theory, Volume III, Durand Reprint, 1943, pp 238-240.

4. $$\left(\frac{z}{\chi}\right)^{\frac{\gamma-1}{\gamma}} = 1 + \frac{\gamma-1}{48\cos^2\beta}\left[(\gamma-1) + (\gamma+1)\left(\frac{z}{\chi}\right)\right]$$

$$\frac{p_1}{p_0} = \frac{1}{\left(1 + \frac{\gamma-1}{2} M_1^2\right)^{\frac{\gamma}{\gamma-1}}} \quad *$$

M_1, the free stream Mach Number is known from the Taylor-Maccoll solution of flow around a cone. $M_s^* = \dfrac{\text{local velocity}}{\text{critical speed of sound}} = \dfrac{W}{a^*}$ is known at various points on the surface of the body and

$$\left(M_s^*\right)^2 = \frac{\gamma+1}{\gamma-1 + \frac{2}{M_s^2}}$$

or

$$M_s^2 = \frac{2 M_s^{*2}}{(\gamma+1) - (\gamma-1) M_s^{*2}}$$

where M_s is the Mach number at any point on the surface of the missile. Substituting for M_s in the equation for p_0/p:

$$\frac{p_0}{p} = \left[1 + \frac{\gamma-1}{2}\left(\frac{2 M_s^{*2}}{(\gamma+1) - (\gamma-1) M_s^{*2}}\right)\right]^{\frac{\gamma}{\gamma-1}}$$

or

$$\frac{p}{p_0} = \left[1 - \frac{(\gamma-1)}{(\gamma+1)} M_s^{*2}\right]^{\frac{\gamma}{\gamma-1}}$$

Substituting these quantities into the expression for C_p:

$$C_p = \frac{2}{\gamma}\frac{\frac{p}{p_0} - \frac{p_1}{p_0}}{\frac{\gamma M_1^2}{2} \frac{p_1}{p_0}}$$

$$C_p = \frac{2}{\gamma}\left[\frac{\left(1 - \frac{\gamma-1}{\gamma+1} M_s^{*2}\right)^{\frac{\gamma}{\gamma-1}} - \left(\frac{1}{1 + \frac{\gamma-1}{2} M_1^2}\right)^{\frac{\gamma}{\gamma-1}}}{\frac{\gamma M_1^2}{2}\left(\frac{1}{1 + \frac{\gamma-1}{2} M_1^2}\right)^{\frac{\gamma}{\gamma-1}}}\right]$$

*Liepmann, H. W., and Puckett, A.E., "Introduction to Aerodynamics of a Compressible Fluid", John Wiley & Sons, 1947, p. 26.

where the only variable for any one free stream M_1 is M_s^*.

The coefficient of drag, C_D, is defined for a three dimensional body:

$$C_D = \frac{1}{d^2} \frac{D}{\frac{1}{2}\rho_0 W^2}$$

where d is the maximum diameter of the body.

$$D = \frac{1}{2}\rho_0 W^2 \int_0^R C_p \, 2\pi r \, dr$$

$$C_D = \frac{1}{d^2} \int_0^R 2\pi r \, C_p \, dr$$

This integral is numerically evaluated with C_p being known from the above equation.

DISCUSSION OF RESULTS

The Sauer Method of Characteristics was applied to the nose section of the Corporal E for free stream Mach numbers of 2 and 4. The shape of the missile was given by the parabola $r = 15\left(1 - \dfrac{x^2}{L^2}\right)$, $L = 96"$. The result for a free stream Mach number of 3 was obtained from a solution for the same nose section by H. K. Forster. For the case of $M = 4$ two entirely independent calculations were made to check the consistency of results. In one of these solutions the nose was assumed to be conical for a distance of six inches from the vertex and the constant velocities obtained from the Taylor-Maccoll solution for a cone were assumed to occur over this portion of the nose. In the second of the computations the nose was assumed to be conical for a distance of nine inches from the vertex. It can be seen from the plot of pressure coefficients obtained in Fig. (8) that the results were consistent.

The pressure coefficients obtained for $M = 2$ and $M = 4$ are tabulated in Tables IV, V and VI and are plotted in Figs. (8) and (9). For comparison, values of C_p, obtained by the Karman Moore Method as applied by W. Z. Chien* to Ogive Nose Sections, are plotted. Figs. (12) and (13). This method makes use of a linearizing process and a close check of results would not be expected. It is noted however that a closer check is obtained at the higher Mach numbers. This is consistent with theory.

Values of the drag coefficients obtained are: At $M = 2$, $C_D = 0.09168$, at $M = 3$, $C_D = .066$, and at $M = 4$, $C_D = 0.061$. These are compared to the values obtained from the Karman Moore Method in Fig. (14).

*Wave Drag of a Projectile Nose at a Supersonic Velocity by the Karman-Moore Method, ORDCIT Report No. 4-24, April 19, 1946.

All of the points computed in the Mach nets are indicated in Figs. (5), (6), and (7), and the velocities and shock wave angles are tabulated in Tables II and III. (In these tables the velocity is expressed in terms of the critical velocity, C^*, $M^* = \dfrac{velocity}{C^*}$)

The calculation of points and of velocities at these points theoretically could be carried out to any desired degree of accuracy depending on the scale used in the graphical solution. Actually the scale used is limited in the hodograph plane by the size of drafting equipment available. In this instance a twenty-four inch rule calibrated in 1/50 inch increments (5 units equal 1 inch) was used. In the M = 4 solution 50 units correspond to $M^* = 1$, and in the M = 2 solution 65 units correspond to $M^* = 1$. These scales were chosen so that the full length of the rule would be utilized (and thus maximum accuracy) in the hodograph plane. In the physical plane 5/3 units correspond to 1 inch (i.e. a 1:3 scale).

Following is an outline of the steps in the solution of M = 4 for the Corporal E nose section:

1. Taylor-Maccoll solution*

   A. A value for U/c corresponding to M = 4 was chosen from the graph.

   B. A tabular form was set up and indicated calculations were made using increments of ϕ equal to 0.5 degrees.

   C. The angle of the shock wave was solved for in the Taylor-Maccoll region as indicated.

   D. The next step was to solve for the exact free stream Mach number.

---

*Taylor, G. I. and Maccoll, J. W., "Air Pressure on a Cone Moving at High Speeds", Proc. of the Roy. Soc., A, Vol. 139, Pages 278-311. 1933.

E. Operations were carried out as indicated in Table VII.

$$M^* = W_{max} \sqrt{\frac{\gamma+1}{\gamma-1}} = 2.437 \, W_{max}.$$

M* was converted to the scale in use.

2. The nose section was drawn to the scale chosen.

3. A shock polar was constructed for Mach number 3.9712 as indicated in Fig. (5).

4. Coordinates of the hodograph plane were drawn above the physical plane in such a position as not to interfere with the Mach net.

5. A table of Mach angles and sine squared of the Mach angle was made for anticipated valocities. (See Table VIII).

$$\frac{1}{M^2} = \sin^2 \alpha = \frac{1 - \frac{\gamma-1}{\gamma+1} M^{*2}}{\frac{2}{\gamma+1} M^{*2}}$$

6. From Taylor-Maccoll's solution velocities were drafted in the hodograph plane and in the physical plane the η lines were drawn using average values of Mach angle between the points. (Point 1 was taken a distance from the nose corresponding to 6 inches in one case and 9 inches in the other).

7. Calculations of the Mach net by the Sauer Method was started. It was advisable to calculate the slope of the nose at the intersection by a ξ line from the geometry of the body rather than to approximate it graphically.

8. When a point on the shock wave had to be found the shock polar was placed over the hodograph plane and was removed after the point was located.

9. Z was calculated. (see Table IX).

10. C_p was calculated. (see Table IV), and a plot of C_p vs. X was made.

11. Even increments of X were taken and the corresponding values of r and C_p were tabulated.

12. A plot rC_p vs. r, see Fig. (10), was made and the "positive" area under this curve was determined. This area was connected to the proper scale. (In this case the conversion factor was $\left(\left(\frac{3}{5} \right)^2 \times 0.4 \right)$.

13 The value for $C_D = \frac{2\pi}{d^2} \times \text{Area}$ was calculated.

It was found that the most efficient method of constructing the Mach net was to work in pairs. One person drafted while the other performed the calculations. From three to ten points per hour were completed after proficiency in the mechanical processes was obtained. The average working speed was about five points per hour.

MACH NET FOR M = 3.9712 (Solution I)
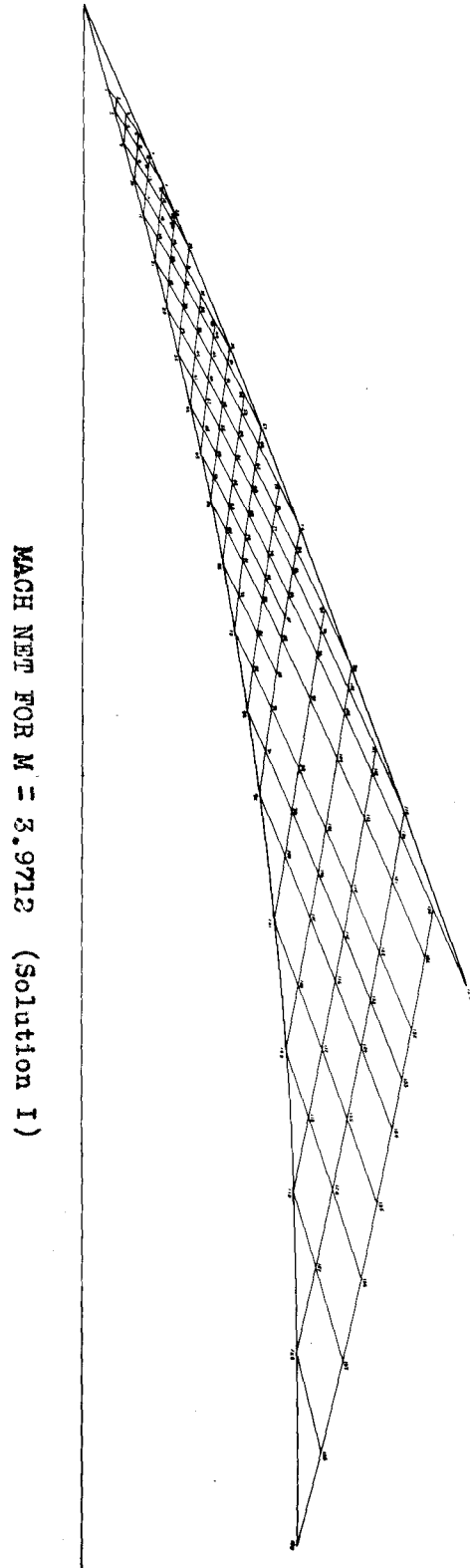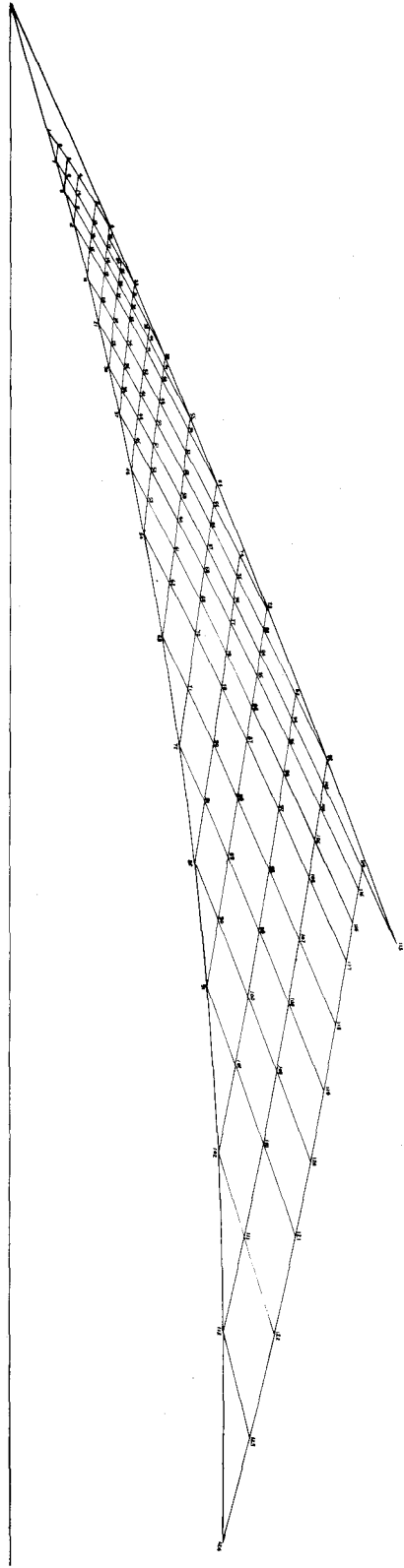
Figure (5)

MACH NET FOR M = 3.9712 (Solution II)

Figure (6)
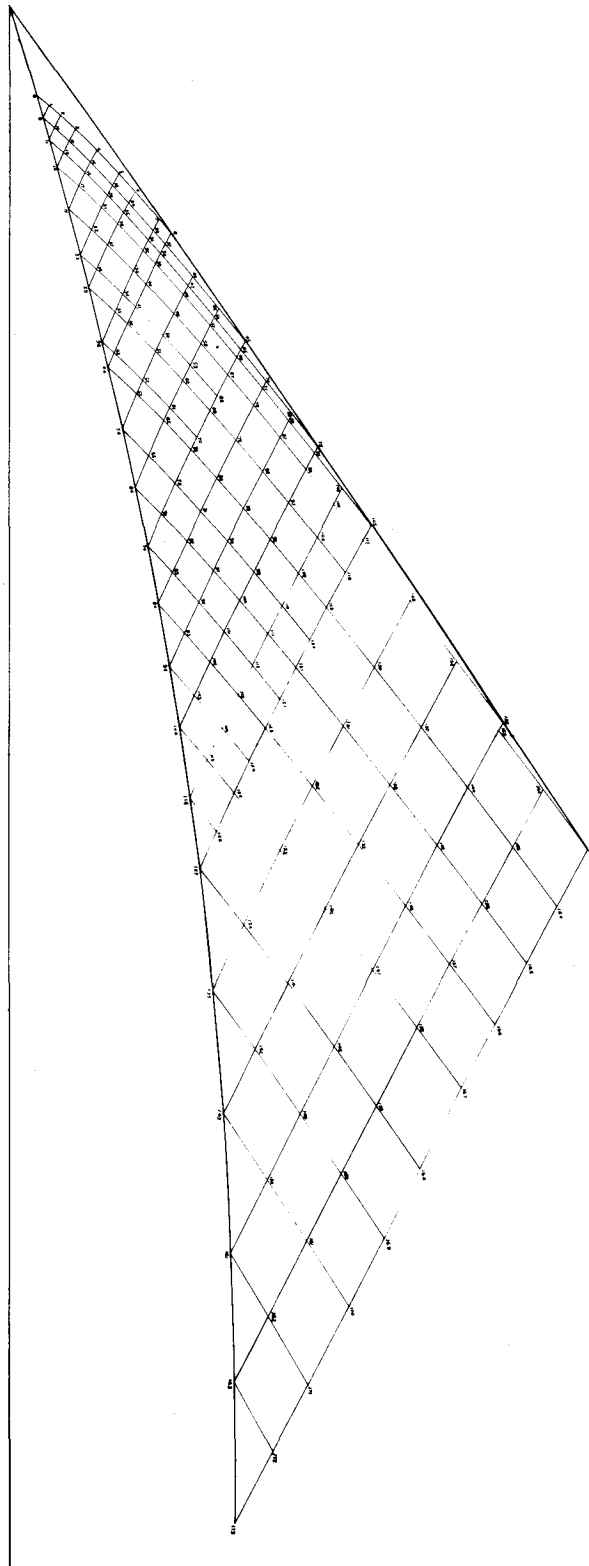
MACH NET FOR M = 2.0039

Figure (7)

PRESSURE COEFFICIENT FOR M = 3.9712
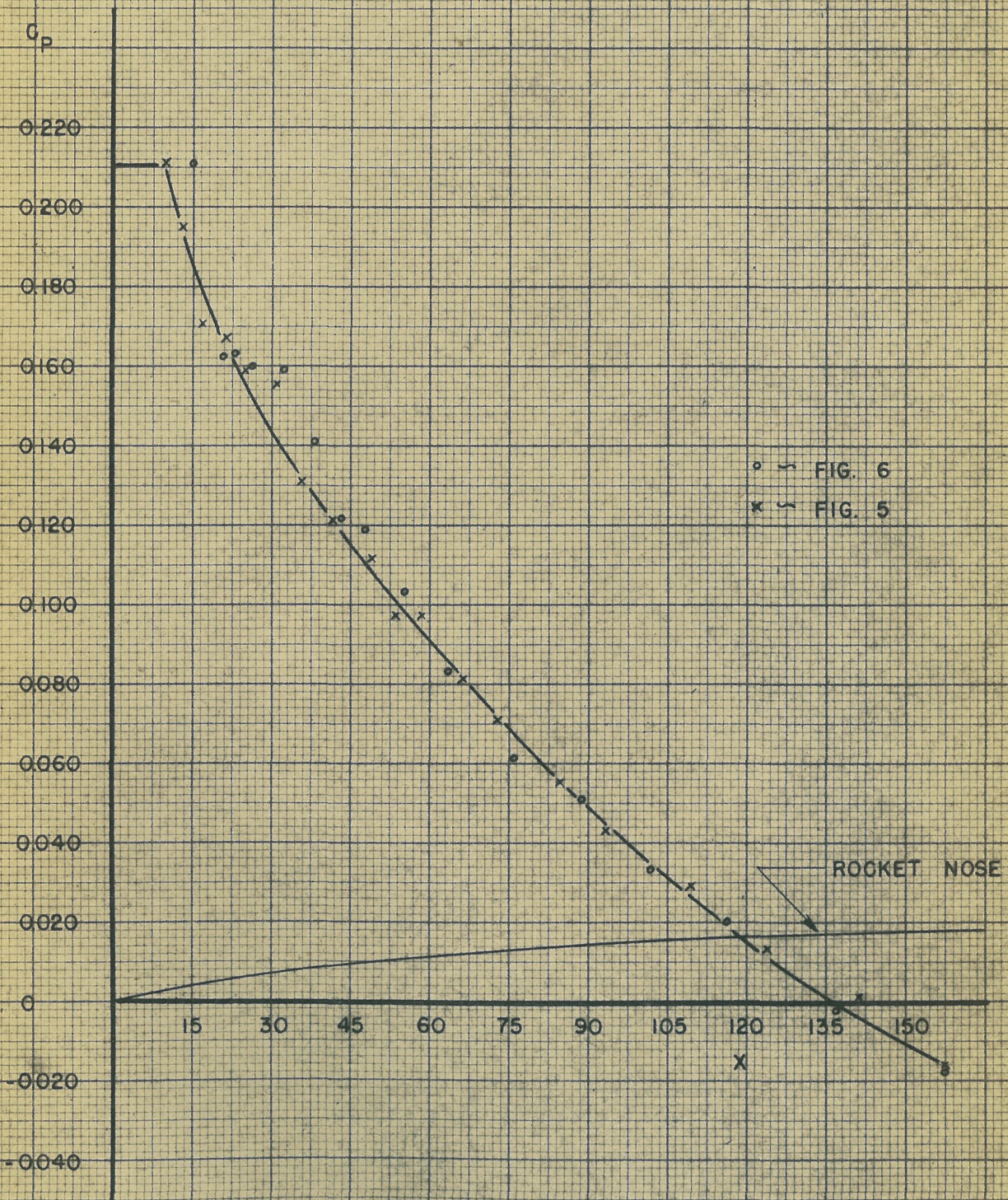
FIGURE 8

PRESSURE COEFFICIENT FOR M = 2.0039
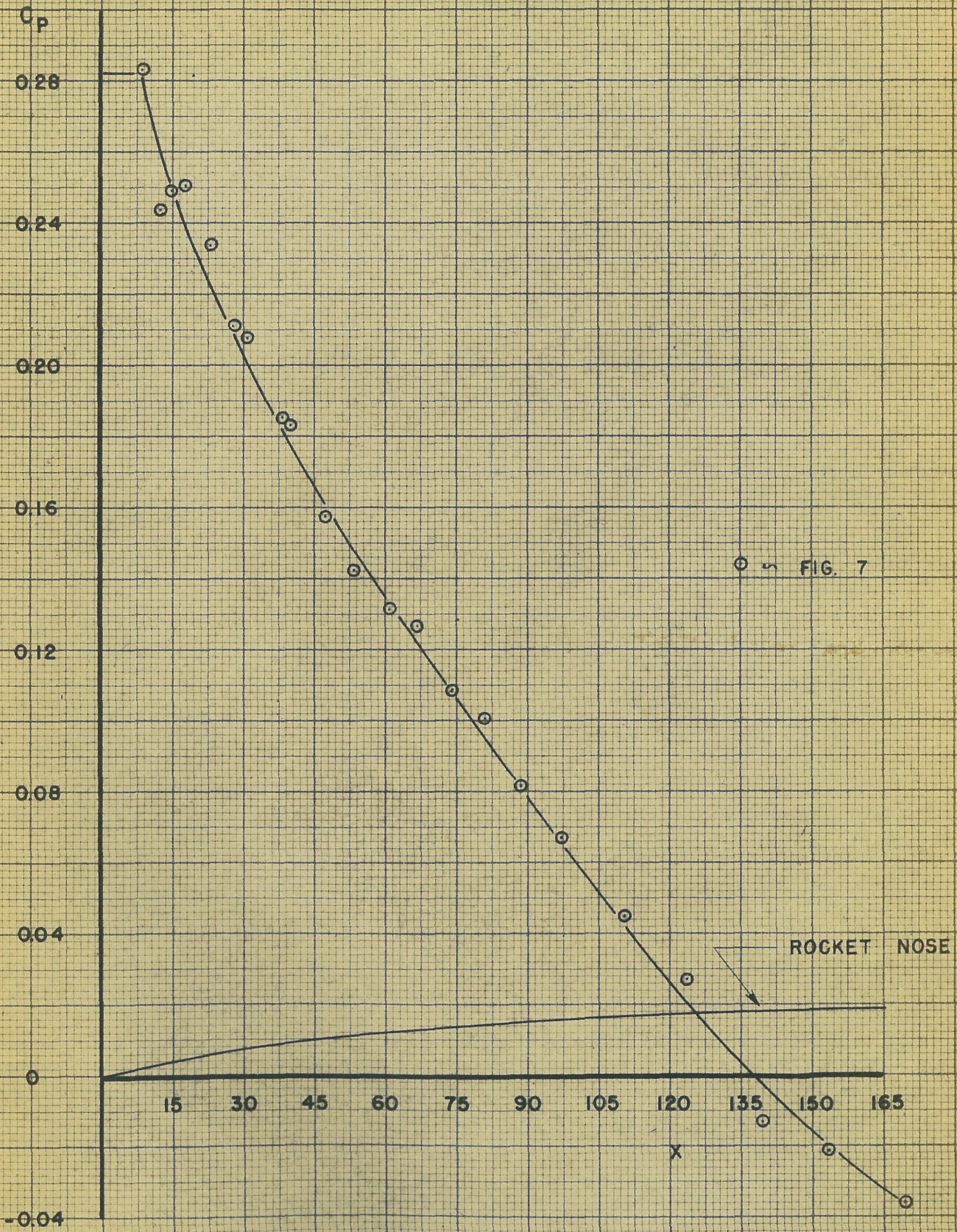
FIGURE 9

$C_p r$ vs r   FOR   M = 3.9712
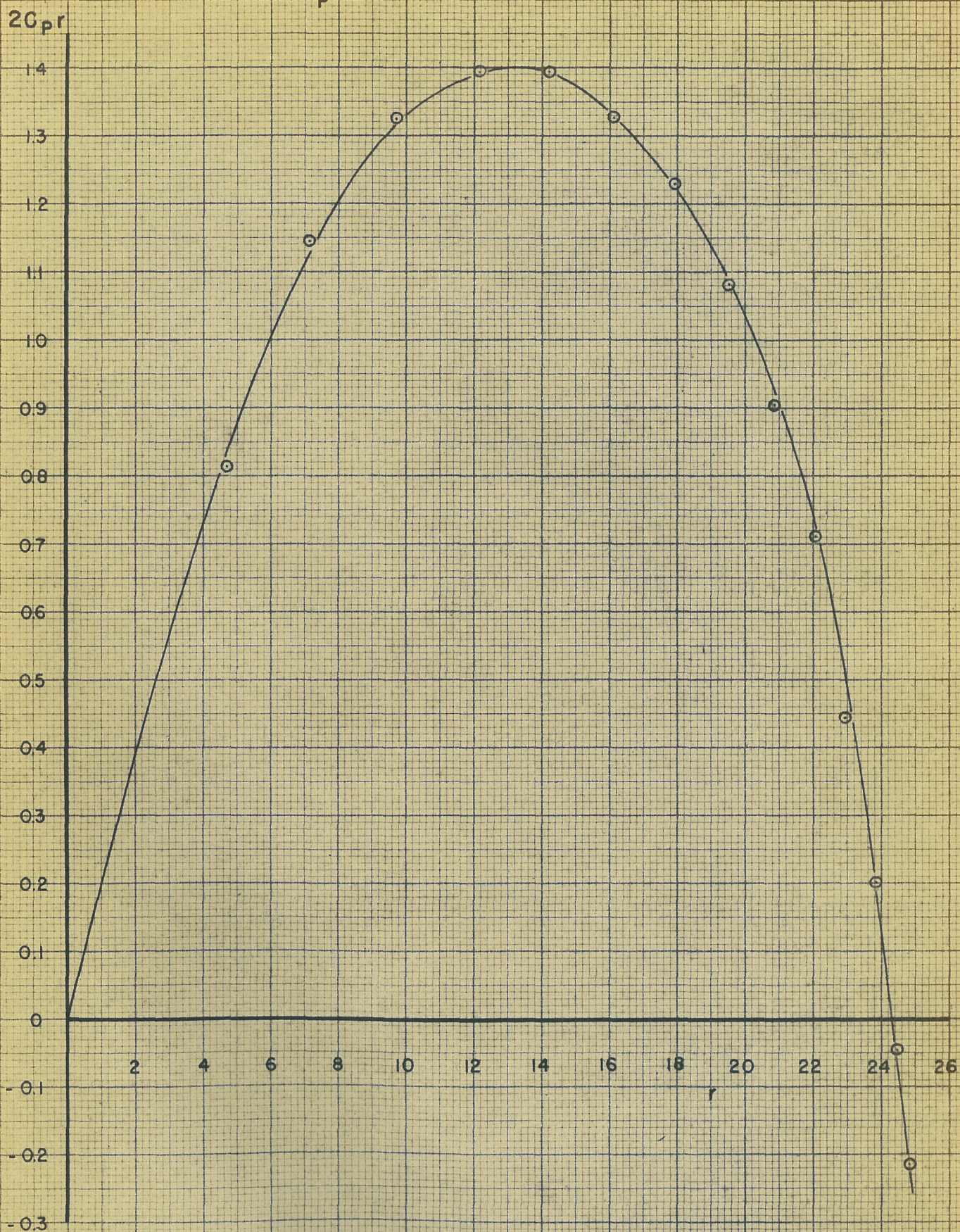
FIGURE 10   (SEE TABLE IV a)

$C_p r$ vs r FOR M = 2.0039
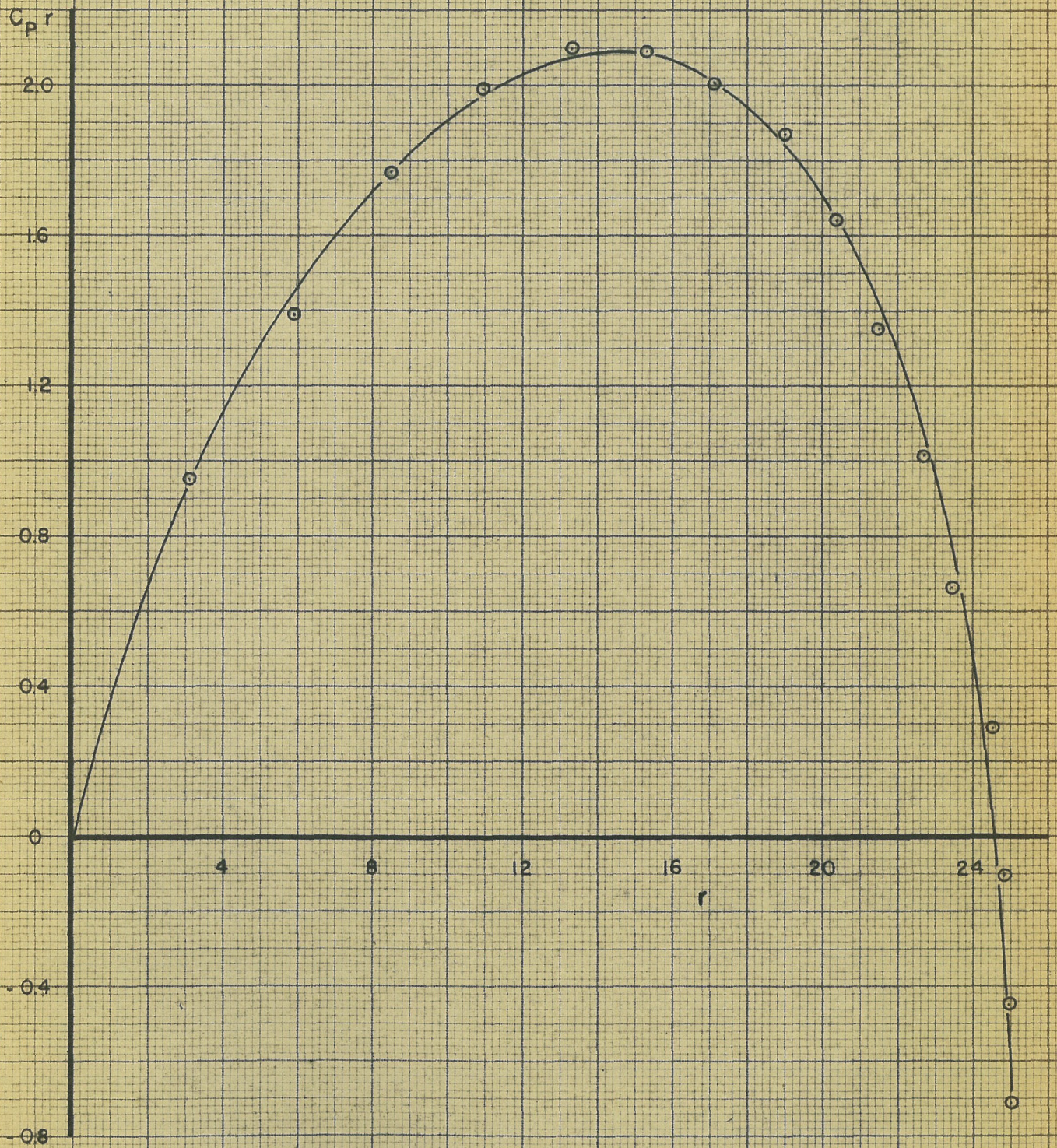
FIGURE 11 (SEE TABLE VI)
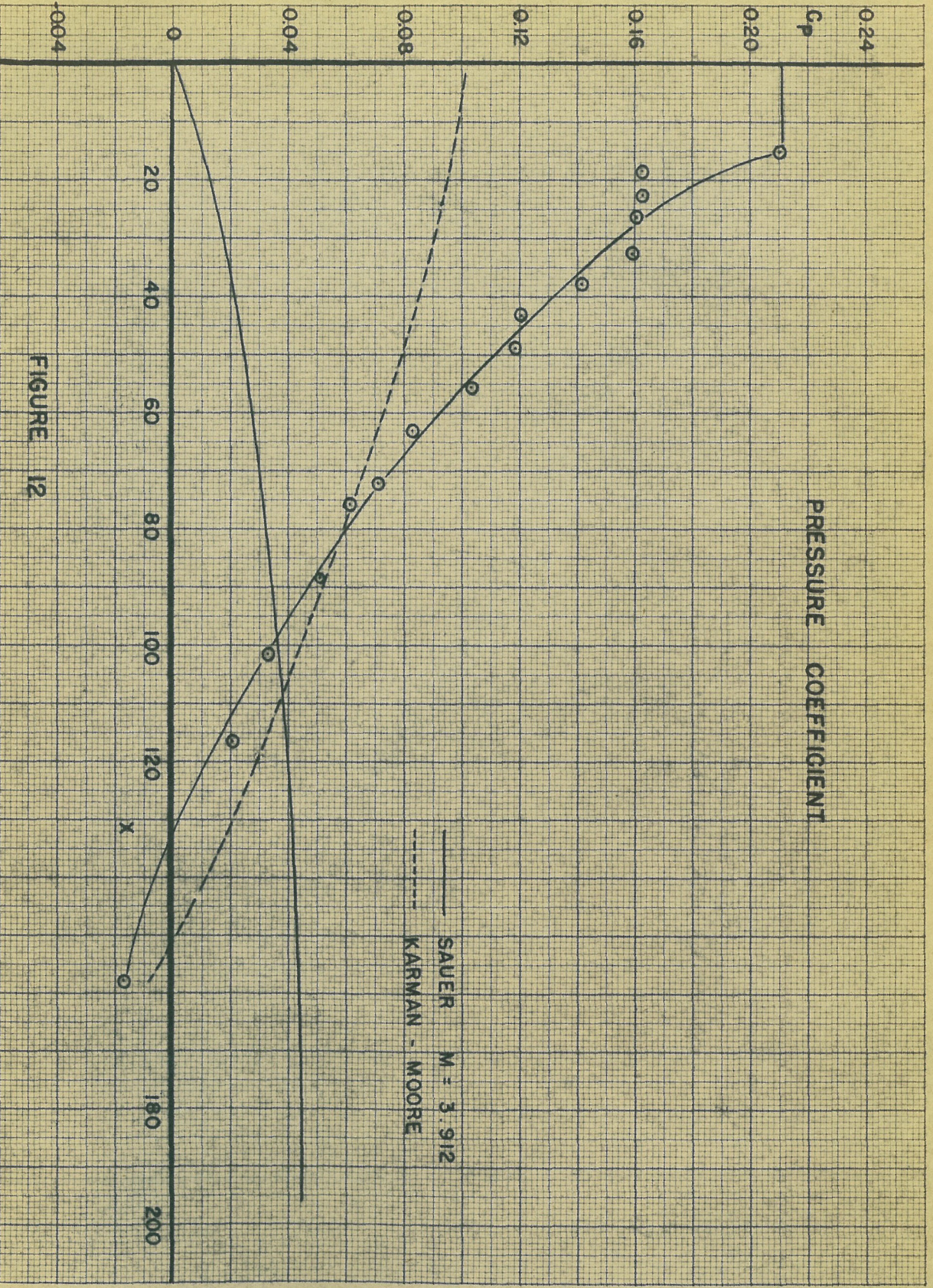
PRESSURE COEFFICIENT

FIGURE 12

——— SAUER   M = 3.912

------- KARMAN - MOORE

C_p

PRESSURE COEFFICIENT

C_P vs X FOR M = 2.0039

SAUER (FROM FIG. 9)

KARMAN - MOORE

FIGURE 13

30_b

C_D vs M

KARMAN - MOORE
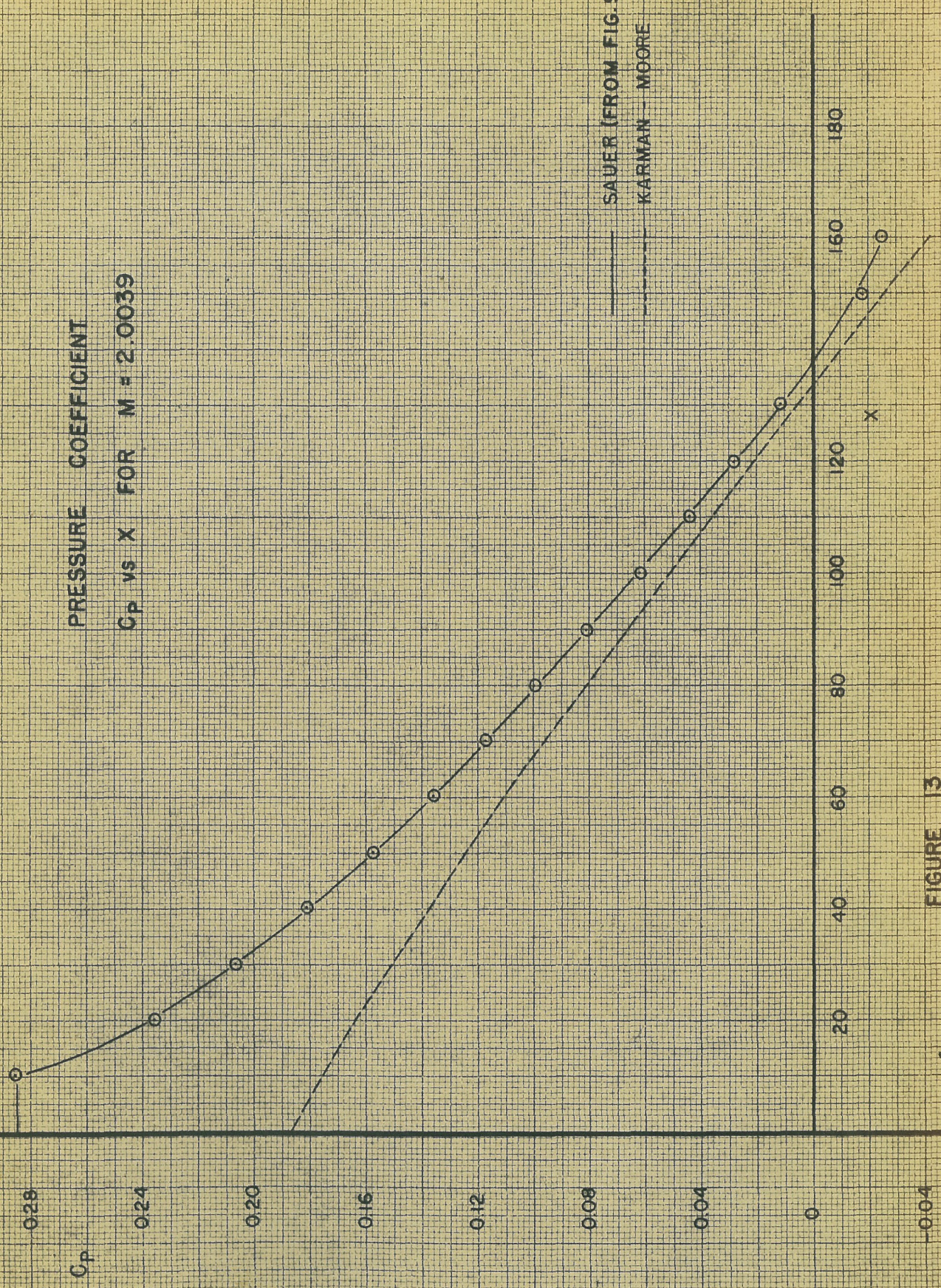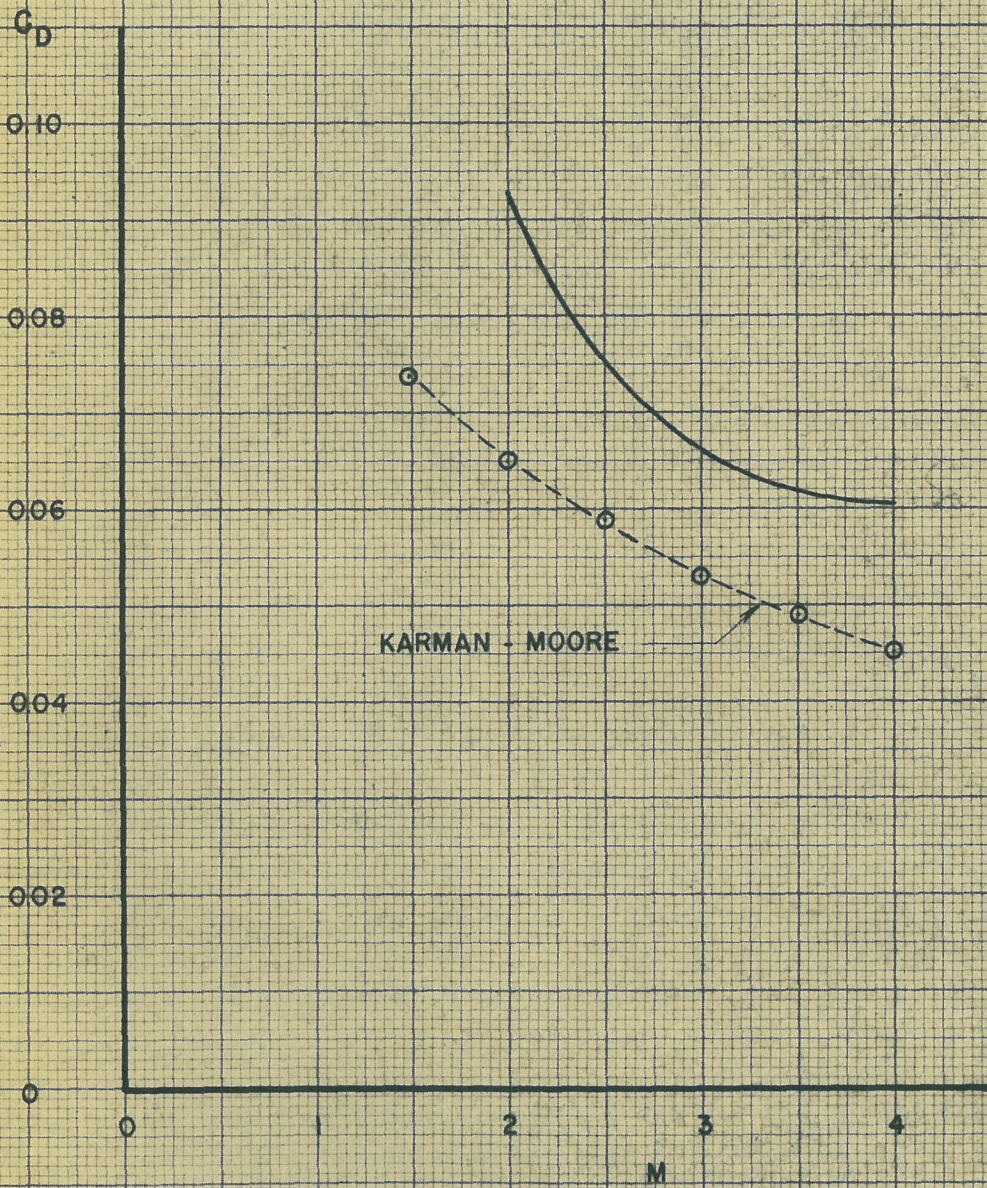
FIGURE 14

In Column 3,
50 units correspond
to M* = 1

TABLE I

SAMPLE TABLE SHOWING DETAILED
CALCULATIONS FOR MACH NET

P	$\overline{P}$	M*	δ		α		$\sin^2\alpha$	ν
			o	'	o	'		
	.69	102.05	9	15				16.35
	₁69 – 68	101.87	9	22	17	9	.0870	16.58
	₁69 – 61	102.05	9	39	17	4	.0862	17.22
69		102.05	9	15				16.35
	.70	102.46	8	50				15.87
	₁70 – 69	102.25	9	2	16	57	.0849	16.11
	₁70 – 62	102.26	9	20	16	56	.0849	16.79
70		102.46	8	50				15.87
	.71	103.12	8	15				14.84
	₁71 – 70	102.79	8	32	16	38	.0819	15.35
	₁71 – 63	103.22	8	50	16	24	.0797	15.96
71		103.16	8	25				15.10
	₁72	103.88	7	58				14.46
	₁72 – 71	103.57	8	11	16	04	.0766	14.78
72		103.75	7	58				14.44
	₁73	101.54	8	44				15.48
	₁73 – 65	101.37	9	14	17	27	.0899	16.10
73		101.54	8	44				15.48
74	₁65 – 73	101.37	9	7				16.10
	₁75	101.48	8	55				15.82
	₁75 – 74	101.42	9	2	17	27	.0899	15.96
	₁75 – 66	101.40	9	27	17	27	.0899	16.32
75		101.50	9	5				16.00
	₁76	101.72	8	52				15.80
	₁76 – 75	101.61	8	58	17	20	.0887	15.90
	₁76 – 67	101.69	9	8	17	16	.0881	16.23
76		101.72	8	52				15.80
	₁77	101.42	9	0				16.04
	₁77 – 76	101.57	8	56	17	21	.0889	15.92
	₁77 – 68	101.56	9	15	17	21	.0889	16.43
77		101.73	8	50				15.90
	₁78	102.00	8	48				15.61
	₁78 – 77	101.87	8	49	17	10	.0872	15.76
	₁78 – 69	102.03	9	02	17	05	.0864	15.98
78		102.00	8	48				15.61

Point 73 is a point on the shock wave. Point 72 is a point on the missile.
All other points are free stream points. P denotes the column for estimated
points. The individual estimated points are designated by ₁( ), ₂( ), etc.
₁( ) – ( ) denotes average values between the indicated points.

TABLE I (Cont'd.)

P	r	$d\xi$	$d\eta$	$d\mu$	dq	∠η o	∠η '	∠ξ o	∠ξ '
	22.40								
	22.65	3.52			.224	26	31	−7	47
	20.87			.485		26	43	−7	25
69	22.40								
	21.83								
	22.11	3.96			.244	25	59	−7	55
	20.31		6.90	.483		26	16	−7	36
70	21.83								
	20.90								
	21.36	6.62			.427	25	10	−8	6
	19.45		6.82	.445		25	14	−7	34
71	20.90								
	19.96								
	20.43	6.90			.381	24	13	−7	53
72	19.96								
	30.34								
	27.18		14.0	.745		26	41	8	13
73	30.34								
74	27.18								
	26.82								
	26.95	2.38			.127	26	29	−8	25
	25.27		6.92	.40		26	54	8	0
75	26.82								
	26.40								
	26.61	2.83			.15	26	18	−8	22
	24.89		6.98	.404		26	24	−8	8
76	26.40								
	26.00								
	26.20	2.65			.143	26	17	−8	25
	24.45		6.90	.412		26	36	−8	6
77	26.00								
	25.50								
	25.75	3.75			.200	25	59	−8	21
	23.95		7.00	.403		26	7	−8	3
78	25.50								

TABLE II (a)
FLOW VELOCITIES FOR

In Column 2
50 units corresponds
to M* = 1

M = 3.9712
SET I

Point	M*	γ °	γ '	Point	M*	γ °	γ '
1	98.60	17	05	46	101.79	11	29
2	98.65	15	44	47	101.07	9	50
3	98.81	14	28	48	100.94	10	10
4	99.05	13	17	49	100.94	10	45
5	99.40	12	07	50	101.03	10	55
6	99.62	11	30	51	101.41	10	50
7	99.93	15	34	52	101.51	11	10
8	99.92	13	53	53	102.00	10	55
9	99.91	15	02	54	102.50	10	49
10	99.95	12	38	55	101.30	9	10
11	99.98	13	37	56	101.18	9	43
12	99.98	14	37	57	101.08	10	07
13	100.17	11	29	58	101.27	10	15
14	100.02	12	15	59	101.51	10	14
15	99.96	13	00	60	101.65	10	15
16	100.08	14	02	61	102.05	10	03
17	100.38	10	41	62	102.50	9	50
18	100.18	11	25	63	103.33	9	25
19	100.10	12	05	64	101.30	9	03
20	100.22	13	00	65	101.20	9	30
21	100.53	13	25	66	101.32	9	32
22	100.00	11	05	67	101.57	9	25
23	100.48	10	15	68	101.70	9	30
24	100.24	10	40	69	102.05	9	15
25	100.60	10	25	70	102.46	8	50
26	100.45	10	53	71	103.16	8	25
27	100.36	11	30	72	103.75	7	58
28	100.45	12	18	73	101.54	8	44
29	100.74	12	40	74	101.37	9	07
30	101.17	12	50	75	101.50	9	05
31	100.82	9	48	76	101.72	8	52
32	100.61	10	30	77	101.73	8	50
33	100.56	11	0	78	102.00	8	48
34	100.55	11	40	79	102.48	8	15
35	100.79	11	53	80	103.10	7	42
36	101.11	12	01	81	103.75	7	24
37	101.25	12	17	82	104.60	6	28
38	101.30	9	10	83	101.71	8	40
39	101.06	9	29	84	101.86	8	33
40	100.79	10	0	85	102.00	8	35
41	100.65	10	34	86	102.30	8	25
42	100.69	11	04	87	102.68	8	0
43	100.88	11	13	88	103.24	7	25
44	101.17	11	17	89	103.78	6	53
45	101.37	11	35	90	104.61	5	53

TABLE II (a) Cont'd.

Point	M*	δ	
		o	'
91	105.24	4	50
92	101.96	8	0
93	101.83	8	20
94	102.00	8	10
95	102.15	8	15
96	102.31	8	0
97	102.70	7	40
98	103.35	7	05
99	103.85	6	25
100	104.65	5	30
101	105.30	4	38
102	106.44	2	40
103	102.13	7	48
104	102.15	7	45
105	102.43	7	48
106	102.78	7	19
107	103.41	6	35
108	103.98	6	01
109	104.75	5	03
110	105.28	4	05
111	106.33	2	21
112	107.49	0	18
113	102.45	7	20
114	102.29	7	34
115	102.44	7	25
116	102.56	7	15
117	102.93	6	53
118	103.43	6	10
119	103.98	5	30
120	104.64	4	30
121	105.25	3	35
122	106.28	1	50
123	107.25	0	12
124	107.18	0	0

In Column 2
50 units corresponds
to M* = 1

TABLE II (h)
FLOW VELOCITIES FOR M = 3.9712
SET II

Point	M*	ϑ °	ϑ '	Point	M*	ϑ °	ϑ '
1	98.60	17	08	46	101.10	11	10
2	98.75	15	18	47	101.45	11	20
3	98.97	13	41	48	101.60	11	45
4	99.40	12	07	49	102.00	11	50
5	99.50	16	05	50	101.00	9	45
6	99.55	13	55	51	101.00	10	25
7	99.70	15	42	52	101.10	10	30
8	99.90	12	10	53	101.40	10	34
9	99.40	14	00	54	101.55	10	45
10	99.80	15	13	55	101.85	10	45
11	99.62	11	30	56	102.00	11	13
12	100.10	11	25	57	101.25	8	50
13	99.55	13	00	58	101.12	9	18
14	99.85	13	50	59	101.10	9	45
15	100.00	14	47	60	101.25	9	50
16	99.86	11	28	61	101.50	10	00
17	100.15	10	30	62	101.60	10	15
18	99.85	11	45	63	101.90	10	20
19	100.00	12	15	64	102.00	10	40
20	100.00	13	15	65	102.60	10	24
21	100.15	14	12	66	101.30	9	15
22	100.05	10	55	67	101.40	9	30
23	100.35	10	15	68	101.65	9	30
24	100.10	11	25	69	101.70	9	45
25	100.20	11	45	70	102.10	9	55
26	100.25	12	25	71	102.20	10	10
27	100.35	13	20	72	102.60	9	55
28	100.90	13	40	73	103.00	9	53
29	100.19	11	02	74	101.60	8	15
30	100.35	10	15	75	101.45	8	45
31	100.35	10	50	76	101.60	8	55
32	100.40	11	40	77	101.70	8	51
33	100.50	12	15	78	101.90	9	07
34	100.90	12	32	79	102.20	8	55
35	101.20	13	02	80	102.30	9	15
36	100.90	9	30	81	102.65	9	00
37	100.53	10	23	82	103.00	9	05
38	100.60	10	45	83	103.60	8	30
39	100.60	11	35	84	101.80	8	25
40	101.00	11	45	85	101.95	8	20
41	101.40	12	0	86	102.00	8	50
42	101.50	12	25	87	102.25	8	45
43	101.72	9	56	88	102.40	8	50
44	100.90	10	12	89	102.70	8	40
45	100.90	10	55	90	103.05	8	30

TABLE II (b) Cont'd.

Point	M*	6 o	'
91	103.60	8	10
92	104.15	7	33
93	102.10	7	35
94	101.95	8	00
95	102.00	8	10
96	102.05	8	15
97	102.30	8	05
98	102.95	7	32
99	103.95	7	00
100	104.00	6	45
101	104.80	5	50
102	102.10	7	50
103	102.20	7	50
104	102.50	7	42
105	103.00	7	00
106	103.55	6	15
107	104.05	6	10
108	104.85	5	15
109	105.55	4	10
110	102.30	7	00
111	102.20	7	25
112	102.40	7	30
113	102.60	7	13
114	103.10	6	40
115	103.65	6	12
116	104.10	5	45
117	104.80	4	45
118	105.50	3	50
119	106.30	2	20
120	102.35	7	10
121	102.65	7	00
122	103.20	6	25
123	103.70	5	55
124	104.10	5	25
125	104.95	4	30
126	105.45	3	38
127	106.30	2	16
128	107.30	0	12
129	102.60	6	50
130	102.48	7	00
131	102.85	6	45
132	103.30	6	20
133	103.80	5	40
134	104.35	5	10
135	105.00	4	05
136	105.65	3	20
137	106.40	2	00
138	107.40	0	05
139	107.50	0	0

In Column 2,
65 units corresponds
to M*= 1

TABLE III
FLOW VELOCITIES FOR M = 2.0039

Point	M*	θ °	θ '	Point	M*	θ °	θ '
1	94.90	13	46	46	99.38	6	13
2	95.65	11	19	47	99.60	6	20
3	96.38	9	47	48	99.05	7	00
4	97.28	8	22	49	99.70	7	55
5	98.01	7	25	50	98.70	8	30
6	99.44	6	55	51	98.65	9	10
7	98.94	6	22	52	98.90	10	20
8	99.19	6	05	53	99.00	11	00
9	96.05	16	03	54	99.69	12	25
10	96.20	12	40	55	99.58	5	56
11	95.90	15	49	56	99.95	5	50
12	96.65	10	35	57	99.40	6	35
13	96.20	12	35	58	99.10	7	20
14	95.85	15	30	59	99.20	7	45
15	97.40	8	55	60	99.10	8	15
16	97.00	10	10	61	99.10	9	5
17	96.30	11	58	62	99.15	9	30
18	96.50	15	00	63	99.70	10	30
19	97.80	8	00	64	100.35	11	43
20	97.65	8	45	65	100.25	5	30
21	97.05	10	05	66	99.80	6	10
22	96.85	12	01	67	99.50	6	50
23	97.30	14	28	68	99.55	7	14
24	98.35	7	25	69	99.45	7	37
25	98.10	8	00	70	99.45	8	12
26	97.50	9	05	71	99.50	8	40
27	97.20	10	35	72	99.90	9	20
28	97.40	12	20	73	100.20	10	00
29	97.55	14	05	74	100.80	11	00
30	98.75	6	50	75	100.80	4	35
31	98.65	7	12	76	100.43	5	12
32	98.15	8	00	77	100.10	5	40
33	97.80	9	15	78	99.80	6	10
34	97.95	10	20	79	99.50	7	00
35	98.00	11	30	80	99.40	7	40
36	98.50	13	28	81	99.85	8	15
37	99.10	6	30	82	100.15	8	50
38	99.00	6	50	83	101.00	9	00
39	98.50	7	40	84	101.00	10	18
40	97.95	8	40	85	100.62	4	54
41	98.15	9	40	86	100.30	5	25
42	98.20	10	25	87	100.10	5	40
43	98.50	12	00	88	99.80	6	30
44	98.60	13	10	89	99.75	7	10
45	99.78	5	40	90	100.05	7	30

TABLE III (Cont'd.)

Point	M*	δ °	δ '	Point	M*	δ °	δ '
91	100.30	7	50	140	102.00	5	10
92	100.95	8	00	141	103.45	4	45
93	100.30	8	55	142	104.45	4	30
94	101.80	9	33	143	105.65	4	06
95	100.50	5	05	144	101.20	4	30
96	100.30	5	25	145	101.35	4	50
97	100.20	5	45	146	101.80	4	55
98	99.85	6	30	147	102.35	5	00
99	100.10	6	50	148	103.75	4	30
100	100.30	7	15	149	104.80	4	05
101	101.20	7	10	150	105.90	3	40
102	100.95	8	00	151	107.80	2	21
103	101.55	8	20	152	101.24	4	08
104	102.20	8	48	153	101.65	3	45
105	100.75	4	30	154	101.44	3	56
106	100.62	4	48	155	101.35	4	10
107	100.50	5	05	156	101.40	4	25
108	100.35	5	25	157	101.80	4	20
109	100.30	6	00	158	102.35	4	20
110	100.40	6	20	159	103.70	3	45
111	100.55	6	40	160	104.65	3	20
112	101.35	6	35	161	105.70	2	50
113	101.20	7	10	162	107.45	1	35
114	101.65	7	30	163	108.20	0	46
115	102.20	7	45	164	101.65	4	00
116	103.05	7	57	165	101.75	4	15
117	100.62	4	48	166	102.10	4	10
118	100.45	5	05	167	102.60	4	05
119	100.45	5	30	168	103.80	4	30
120	100.50	6	00	169	104.70	3	00
121	100.60	6	15	170	105.70	2	30
122	101.40	6	00	171	107.40	1	12
123	101.35	6	35	172	108.25	0	45
124	101.65	6	50	173	109.00	0	00
125	102.00	7	05				
126	102.80	7	05				
127	103.75	7	05				
128	101.25	4	05				
129	100.83	4	34				
130	100.75	5	10				
131	100.80	5	35				
132	101.40	5	50				
133	102.05	6	05				
134	103.60	5	50				
135	104.80	5	37				
136	100.04	4	20				
137	100.70	4	35				
138	100.80	5	00				
139	101.35	5	10				

TABLE IV
DATA SHEET
FOR CALCULATION
OF C_p FOR M = 3.9712
(CORRESPONDING TO FIG. (6).

Point	Coordinates		50 M*	M*	C_p	$2rC_p$
	χ	λ				
1	15	4.36	98.60	1.9720	.2109	1.83905
7	18.83	5.48	99.93	1.9986	.1621	1.97662
9	22.32	6.45	99.91	1.9982	.1634	2.10786
12	26.23	7.49	99.98	1.9996	.1604	2.40279
16	32.62	9.15	100.08	2.0016	.1596	2.92068
21	37.96	10.45	100.53	2.0106	.1419	2.96571
30	43.19	11.67	101.17	2.0234	.1218	2.84281
37	48.74	12.96	101.25	2.0250	.1192	3.08966
46	55.48	14.34	101.79	2.0358	.1032	2.95978
54	63.05	15.78	102.50	2.0500	.0833	2.62895
63	75.20	18.00	103.33	2.0666	.0619	2.22840
72	88.17	19.96	103.75	2.0750	.0519	2.07185
82	101.97	21.75	104.60	2.0920	.0330	1.43550
91	116.63	23.12	105.24	2.1048	.0201	0.92942
102	136.40	24.46	106.44	2.1288	-.0016	-0.78272
112	157.52	24.98	107.49	2.1498	-.0178	-0.88929
124	182.10	25.00	107.18	2.1436	-.0133	-0.66500

TABLE V
DATA SHEET FOR CALCULATION OF C_p FOR M = 3.9712

CORRESPONDING TO FIG. (5)

Point	x	R	50 M*	M*	C_p	rC_p
1	10	3.03	98.6	1.972	.2109	.6390
5	12.60	3.80	99.5	1.980	.1957	.7436
7	16.20	4.75	99.70	1.994	.1701	.8079
10	20.60	6.00	99.80	1.996	.1666	.9996
15	24.85	7.10	100.00	2.000	.1597	1.1333
21	30.20	8.45	100.15	2.003	.1546	1.3063
28	35.60	9.75	100.90	2.018	.1301	1.2684
35	41.15	11.10	101.20	2.020	.1207	1.3397
42	47.20	12.50	101.50	2.030	.1116	1.3950
49	52.80	13.80	102.00	2.040	.0971	1.3400
56	58.30	14.95	102.00	2.040	.0971	1.4516
65	65.90	16.40	102.60	2.052	.0806	1.3218
73	73.70	17.70	103.00	2.060	.0702	1.2425
83	83.30	19.30	103.60	2.072	.0554	1.0692
92	93.00	20.65	104.15	2.083	.0428	.8338
101	107.80	22.30	104.80	2.096	.0287	.6400
109	122.80	23.70	105.55	2.112	.0132	.3128
119	139.10	24.60	106.30	2.126	.0007	.0172
128	157.65	24.85	107.30	2.146	-.0151	-0.3752
139	180.80	25.00	107.50	2.150	-.0179	-0.4475

TABLE VI
DATA SHEET FOR CALCULATION OF C_p FOR M = 2.0039

CORRESPONDING TO FIG. (9)

Point	x	r	65 M*	M*	C_p	rC_p
0	10.00	3.08	94.57	1.454922	.28291	0.871
9	12.40	3.80	96.05	1.477692	.24400	0.927
11	15.00	4.50	95.90	1.475384	.24292	1.121
14	18.00	5.35	95.85	1.474615	.25051	1.340
18	22.80	6.65	96.50	1.484615	.23419	1.557
23	27.90	7.95	97.30	1.496923	.21442	1.705
29	31.50	8.85	97.55	1.500769	.20831	1.844
36	37.60	10.30	98.50	1.515538	.18513	1.907
44	40.50	11.00	98.60	1.516923	.18299	2.013
54	47.30	12.60	99.65	1.533076	.15822	1.994
64	53.80	14.00	100.35	1.543846	.14205	1.989
74	60.50	15.40	100.80	1.550769	.13178	2.029
84	67.00	16.55	101.00	1.553846	.12724	2.106
94	74.00	17.80	101.80	1.566153	.10934	1.946
104	80.80	18.90	102.20	1.572307	.10053	1.900
116	88.70	20.10	103.05	1.585384	.08205	1.649
127	96.40	21.10	103.75	1.596153	.06732	1.420
135	110.00	22.60	104.80	1.612307	.04528	1.023
143	123.60	23.90	105.65	1.625384	.02805	0.670
151	139.10	24.70	107.80	1.658461	-.01373	-0.339
163	153.20	25.00	108.20	1.664615	-.02122	-0.531
173	168.80	25.00	109.00	1.676922	-.03592	-0.898

TABLE VII
TAYLOR-MACCOLL: M = 2.0039
VELOCITIES AT A MISSILE TIP FROM TAYLOR-MACCOLL SOLUTION

ϕ	$-v$	u	M*	$\propto$		$-\frac{v}{u}$	$-\phi'$		ζ		$\angle\eta$	
				o	'		o	'	o	'	o	'
17.08	0	.59700	1.4549	37	12	0	0		17	5	54	17
19.00	.03852	.59635	1.4564	37	8	.06459	3	42	15	18	52	26
21.00	.07538	.59435	1.4600	36	56	.12683	7	14	13	46	50	42
23.00	.10992	.59111	1.4651	36	44	.18595	10	32	12	28	49	12
25.0	.14283	.58670	1.4715	36	26	.24344	13	41	11	19	47	45
26.5	.16674	.58265	1.4768	36	15	.28618	15	58	10	33	46	47
28.0	.19017	.57798	1.4829	35	56	.32902	18	13	9	47	45	43
29.5	.21328	.57210	1.4892	35	39	.37241	20	26	9	4	44	43
31.0	.23626	.56682	1.4966	35	20	.41682	22	38	8	22	43	42
32.0	.25162	.56257	1.5019	35	8	.44727	24	6	7	54	43	02
33.0	.26713	.55804	1.5078	34	51	.47869	25	35	7	25	42	16
34.0	.28295	.55325	1.5144	34	34	.51143	27	5	6	55	41	29
35.0	.29938	.54818	1.5222	34	14	.54613	28	38	6	22	40	36
36.0	.31711	.54280	1.5319	33	50	.58421	30	18	5	42	39	32
35.333)	.30596	.54639	1.5260	34	05	.55997	29	15	6	05	40	10

angle of shock wave

ϕ = geometrical angle selected for Taylor-Maccoll solution

ϕ' = arctan

TABLE VIII

VELOCITIES AT MISSILE TIP FROM TAYLOR-MACCOLL SOLUTION M = 3.9712

ϕ	v^2	u^2	M*	α ° '	$-\dfrac{v}{u}$	$-\phi'$ ° '	δ	$\angle \eta$ ° '
18	.00066	.65448	1.97253	19 04	.031656	1 49	16 11	35 15
20	.006117	.651540	1.97637	18 57	.096893	5 32	14 28	33 25
22	.01656	.64571	1.98324	18 44	.16013	9 05	12 55	31 39
23.5	.02784	.63950	1.99081	18 27	.20865	11 47	11 43	30 10
23.375								30 21
19	.00427	.65256	1.97507	18 59	.06475	3 42	15 18	34 17
21	.01072	.64898	1.97938	18 51	.12853	7 19	13 41	32 32
23	.02371	.64175	1.98801	18 36	.19221	10 53	12 07	30 43

ϕ = geometrical angle selected for Taylor-Maccoll solution

ϕ' = arctan $\dfrac{v}{u}$

BIBLIOGRAPHY

1. Liepmann, H. W., and Puckett, A. E., "Introduction to Aerodynamics of a Compressible Fluid", John Wiley & Sons, 1947

2. Puckett, A. E., "Supersonic Nozzle Design for Engineers", May, 1946

3. Heybe, "The Prandtl-Busemann Method for the Graphical Evaluation of Two-dimensional Supersonic Flow, its Application to the Design of a Wind Tunnel Nozzle and the Appropriate Corrections", Kochel Report 55/56, February 4, 1941.

4. Sauer, R., "Theoretische Einfuhrung in die Gasdynamik", Berlin Springer, 1943

5. Poritsky, H., & others, "Sauer's Graphical Numerical Method for Supersonic Axially Symmetric Flows and its Application to Pressure Distribution on Boat Tail Shapes." General Electric Report #45777, June 26, 1946

6. Taylor, G. I. and Maccoll, J. W., "Air Pressure on a Cone Moving at High Speeds", Proceedings of the Royal Society, Vol. 139, pp 278-311. 1933

7. Durand, W. F., Aerodynamic Theory, Volume III, Durand Reprint, 1943

8. Chien, W. Z., "Wave Drag of a Projectile Nose at a Supersonic Velocity by the Karman-Moore Method." ORDCIT, Report #4-24, April 19, 1946